Severity of Crowding at Evacuation Shelters after a Major Earthquake

Toshihiro Osaragi
Tokyo Institute of Technology
osaragi.t.aa@m.titech.ac.jp

Koji Ogino
Tokyo Institute of Technology
ogino.k02@gmail.com

Noriaki Hirokawa
Tokyo Institute of Technology
hirokawa.n.aa@gmail.com

Takuya Oki
Tokyo Institute of Technology
oki.t.ab@m.titech.ac.jp

ABSTRACT

A number of residents are presumed to evacuate to shelters after a large earthquake. However, the congestion of evacuation shelters has not been enough discussed. In this paper, we propose an evacuation behavior model, which includes sub-models on building damage, water-supply failure, power failure, fire damage, and elevator stall. Using the model estimated using the survey data of the past earthquakes, we discuss the congestion of evacuation shelters under the assumption of Tokyo Bay northern earthquake. Finally, we discuss improvement of water pipes for earthquake resistance to reduce the congestion degree of evacuation shelters, which varies according to regional vulnerability.

Keywords

large earthquake, evacuation shelter, building damage, water-supply failure, simulation, evacuation behavior.

INTRODUCTION

A northern Tokyo Bay earthquake (M7.3) is expected to force approximately 3,390,000 people out of their homes (to become shelter residents) throughout the Tokyo area, and of these, about 2,200,000 people, will be forced to become shelter residents (Tokyo Metropolitan Government, 2015).

Using these estimates, the Tokyo Metropolis has designated primary and secondary shelters that can house a maximum of approximately 3,280,000 persons (Tokyo Metropolitan Government, 2018). In order to minimize confusion and trouble at those sanctuaries, they must first be established, and then refugee preparations must be considered based on the severity of crowding that would be expected at each of the respective shelters. However, it cannot be taken for granted that there will be an appropriate balance among the shelters in terms of levels of local physical damage, numbers of shelter residents, and the scale of each shelter itself. In particular, the spatial distribution of all these factors must be considered. Thus, it is extremely difficult to foresee the severity of crowding at any one shelter.

Among the existing reports on shelters is the detailed survey published by Sakata et al. (1997), in which they analyzed the evacuations in Nada Ward of Kobe City after the southern Hyogo Prefecture earthquake of 1995. This report is interesting in that it describes the characteristics of the various evacuation zones, which differed in their family types: some zones were home mostly to older adults, while others had a preponderance of households with infants or small children, etc. It also provided information from evacuees on how the zones had influenced their choices of shelters. These factors were the individuals' typical daily activities, the consciousness of the presence of the shelters, etc. In a separate study, Seto et al. (2016) employed statistics on crowding based on the location information of cell phone users to estimate the numbers of people present in the shelters at one-hour intervals after the 2016 Kumamoto Earthquake. By making comparisons with the numbers of people present in the shelters during ordinary times, they showed where and to what extent crowding had occurred.

However, most existing studies discuss problems and arrangements in shelters during the crowded period after a disaster (such as meals, hygiene, and relief supplies); also, they typically survey a small number of shelters.

In this paper, we assume that an earthquake has occurred directly under northern Tokyo Bay and analyze the effect on the Tokyo ward area (the 23 wards of the Tokyo Metropolis) itself. We examine the extent of physical damage, and as a result, what number of evacuees will appear at shelters, when and which shelters they flee to, how crowded the shelters become, and how the situation continues to unfold. We also propose and validate measures to reduce the number of shelter residents and to efficiently and effectively minimize shelter crowding. As an example, we demonstrate that it is effective to promote seismic retrofitting of water pipes, in order to reduce the number of evacuees caused by water pipe failure. However, it is impossible to promote seismic retrofitting of water pipes in all areas within a limited budget, and it is not efficient in terms of preparing for an imminent large earthquake. Hence, by conducting experiments using the simulation model constructed in this paper, we will examine the effectiveness of seismic retrofitting of water pipes.

CONSTRUCTION OF PHYSICAL DAMAGE MODEL

Figure 1 shows the outline of physical damage model composed of some sub-models, namely, building damage model, fire damage model, model of water-supply failure, model of power failure, and elevator stall model.

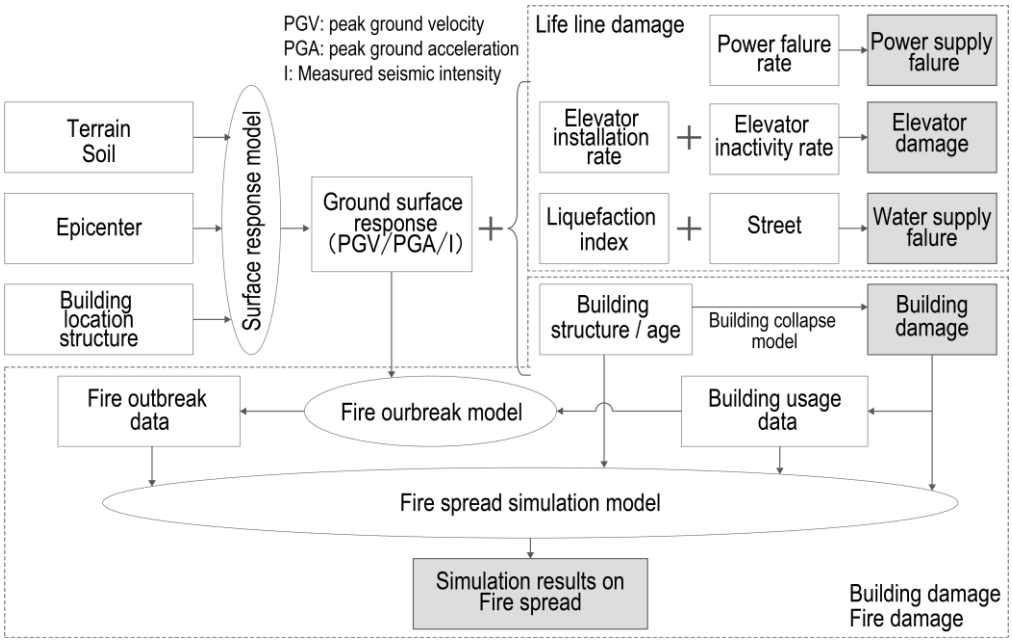

Figure 1. Outline of physical damage model

Building Damage Model

In this study, we adopt the fragility curve for estimating building damage in the model developed by Murao and Yamazaki (2000) based on damage survey data taken after major earthquakes in the past. The significant advantages of this model are that the needed data are available without too much difficulty and that it allows estimates of building damage over a wide area. Osaragi et al. (2015), Hirokawa and Osaragi (2016) describe the data used and the process of calculations in detail.

Fire Damage Model

This study uses a building type fire risk model in which the probability of a fire outbreak is calculated for each building individually, based on various factors. This model was constructed by Tokyo Fire Department (1993, 2005) based on precise investigations on previous disasters and literature reviews on academic research. These include ownership frequency of all kinds of high-temperature equipment such as electric heaters and gas-fired cooking stove burners, which vary with the building type; usage of each type of equipment in each season and at each hour of the day; and the probability of a fire outbreak from any given type of high-temperature equipment estimated for given earthquake magnitudes. The damage in urban regions caused by the spread of fires from their outbreak locations (fire damage) is estimated using a fire spread simulation model constructed by Hirokawa and Osaragi (2017a), who combined a fire spread speed model (Tokyo Fire Department, 1993, 2001) and the distance limit of the fire spread (Iwami et al., 2006).

Model of Water Supply Failure

Overview of water supply failure simulation

Previous estimates of water supply failures after a major earthquake (Tokyo Metropolitan Government, 2015) have considered municipal regions divided into spatial grid cells, but this method is inconvenient when accounting for the characteristics of pipe networks during water supply failures. For example, when a given water pipe ruptures, only users on the downstream side suffer water supply failure; network users between the break and the supply side (upstream of the break) are unaffected. However, this characteristic was not taken into account in previous estimates. Therefore, in this study, the water supply failure simulation model for fire hydrants constructed by Hirokawa and Osaragi (2017b), which takes water pipe networks into consideration, was expanded to predict water supply failures in individual buildings. The model of water supply failure developed in this study should be analyzed carefully. However, we omitted its detailed process, since the original model, the water supply failure simulation model for fire hydrants, was already well analyzed and examined.

Approximation of water pipe network

Although GIS data for Tokyo's water pipe network have not been publicly revealed for reasons of security, Kobayashi et al. proposed a way to approximate this network by using the street network data, since water pipes, gas pipes, and other infrastructure are commonly buried beneath streets (Kobayashi et al., 2013). They showed that the water pipe network could be guessed with high accuracy in densely inhabited districts (DIDs), aside from locations such as overpasses, underpasses, private roadways, etc. With that point in mind, since the entire Tokyo ward area is a DID, this paper will use their procedure to approximate the water pipe network. The pipes will be assumed to be laid in a tree network, where the roots are the water supply facilities. However, since water pipe networks are laid in a grid pattern to eliminate supply failures when trouble occurs in one location, in this report, multiple tree networks originating from different water supply facilities will be overlapped to mimic this redundancy.

Next, in order to approximate a water supply failure while accounting for water supply network characteristics, the water supply facilities were connected to buildings with the water pipe network, and the direction of water flow was set to be away from the water supply facilities to the buildings. This supply is assumed to be conducted by the shortest path (shortest length of pipe) through the network in accordance with a network search algorithm (Dijkstra's algorithm) (Fig. 2).

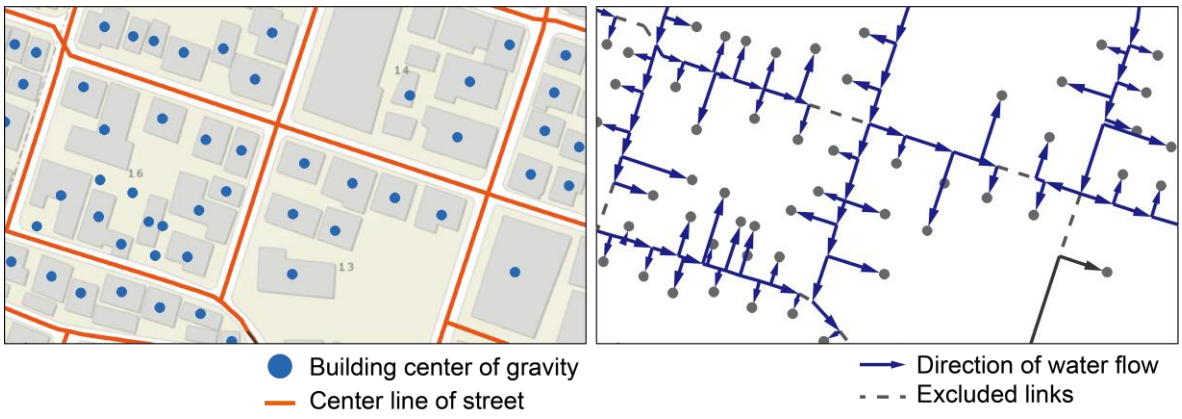

Figure 2. Data used for estimation of structure of pipeline network and direction of water flow

Model of probability of rupture of water pipes

According to the Tokyo Metropolitan Government, the number of expected ruptures $E_D(P_i,E)$ in pipe P_i, given earthquake strength E, is calculated as follows (Tokyo Metropolitan Government, 2015);

$$E_D(P_i,E) = 2.24\times10^{-3}\times C_{PL}(P_i)\times C_D(P_i) \times (PGV(P_i,E)-20)^{1.51}\times L(P_i) \quad (1)$$

where $L(P_i)$ is the length of the pipe [km], $C_D(P_i)$ is a correction coefficient for pipe P_i depending on its type and

diameter (Table 1), and $PGV(P_i,E)$ and $C_{PL}(P_i)$ are the maximum ground velocity [cm/s] at the location of P_i and the correction coefficient for the liquefaction index (*PL* value) (Table 2). The number of expected ruptures $E_D(P_i,E)$ of the water pipe depends on the type of water pipe and the diameter of the pipe. $C_D(P_i)$ is the value to adjust the difference due to the type and diameter of water pipe. The higher this value, the larger number of damaged parts of the water pipe will increase. This model was constructed by Tokyo Fire Department (2015) based on precise investigations on previous disasters and literature reviews on academic research. The liquefaction index (*PL* value) is calculated from the safety rate to liquefaction for every depth derived from drilling data, geology sections and conditions of geomorphological unit. The *PL* value is adopted in earthquake damage assessment of many local governments in Japan.

Table 1. Correction coefficient $C_D(P_i)$ by pipe diameter (road width)

Road width	～ 6 m	6 m～ 8 m	8 m～ 10 m	10 m～
Estimated value of pipe diameter	～ 75 mm	100 mm ～ 450 mm	500 mm ～ 900 mm	1,000 mm～
Ductile cast iron pipe (with seismic coupling)	0.0	0.0	0.0	0.0
Ductile cast iron pipe (without seismic coupling)	0.6	0.3	0.09	0.05

Table 2. Correction coefficient $C_D(P_i)$ by liquefaction risk rank

PL value	Correction coefficient
$PL = 0$	1.0
$0 < PL \leqq 5$	1.8
$5 < PL \leqq 15$	3.2
$15 < PL$	8.8

Next, assuming that the probability of rupture is uniform and independent throughout the various locations, the probability $P_D(P_i, k, E)$ of the number of ruptures k of pipe P_i, given earthquake strength E, is given by the Poisson distribution;

$$\begin{aligned} P_{DL}(P_i,E) &= 1 - P_D(P_i,0,E) \\ &= 1 - \exp\left[-E_D(P_i,E)\right] \end{aligned} \tag{2}$$

Thus, we can express the probability $P_{DL}(P_i, E)$ that at least one break will occur in water pipe P_i of length L [km] using $E_D(P_i,E)$ in the following expression (Hirokawa and Osaragi, 2017b);

$$P_D(P_i,k,E) = \frac{(-E_D(P_i,E))^k \exp\left[-E_D(P_i,E)\right]}{k!} \tag{3}$$

However, since it is difficult to obtain precise values for the *PL* value from boring data at all of the locations, the image data for the liquefaction indices published in the Estimate of Earthquake Damage in Tokyo (Tokyo Metropolitan Government, 2015) (grid cell size = 250 m) were used (Fig. 3). It is also difficult to obtain data about the correction coefficient $C_D(P_i)$ for pipe type and diameter, so the pipe was assumed to be the most common type, ductile cast iron (without seismic joints). Pipe diameter was set according to roadway width (Table 1).

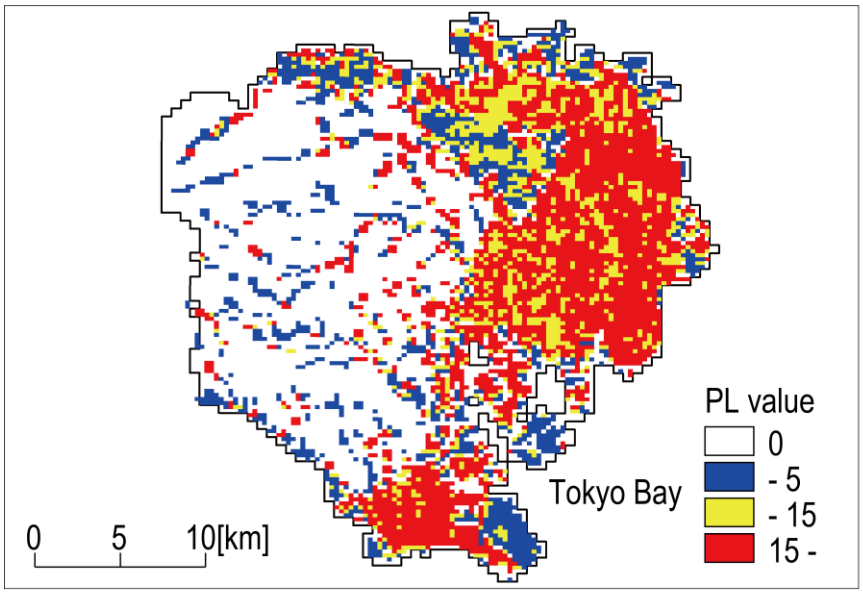

Figure 3. Estimated liquefaction index (*PL* value) based on damage estimate by Tokyo Metropolitan Government

Prediction of buildings affected by water supply failure, according to reachability analysis

The buildings to be affected by a water supply failure were predicted by first estimating the pipe rupture locations using the probability of rupture of water pipe model, and then determined by the possibility of water reaching the building from the water supply facilities (via a network analysis) (Fig. 4). Actually, this is also affected by the level of damage (leakage, pressure losses, water supply failure), but those factors are neglected here to preserve the simplicity of the model.

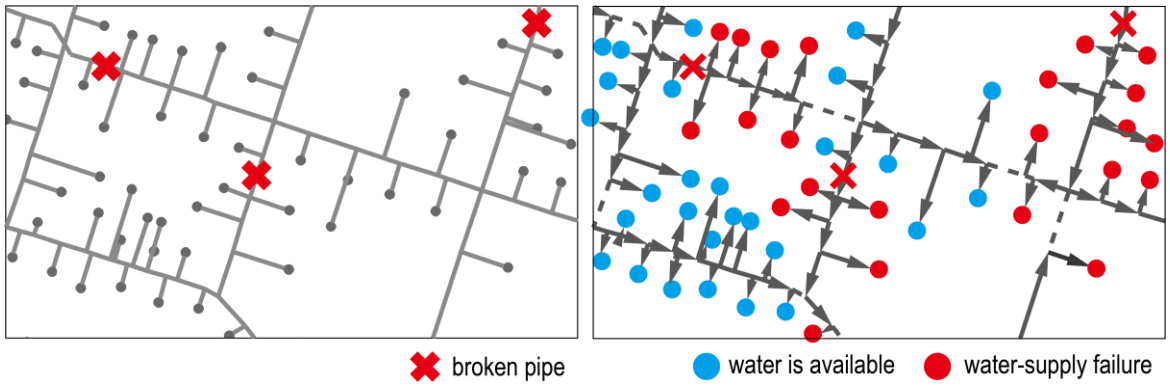

Figure 4. Estimation of broken pipes and buildings with water-supply failure by reachability judgment analysis

Model of Power failure

A power failure is estimated using the power failure rates (Fig. 5) for each ward published by the Tokyo Metropolitan Government (Tokyo Metropolitan Government, 2015). Specifically, the rates were employed with uniform random numbers to determine stochastically whether each building in a given ward would be affected by power failure. As shown in Fig. 5, the model of power failure is not as accurate as other models from the view point of spatial accuracy. To the extent of the information currently available, this is the limitation of this model. The credibility of this model should be scrutinized using the abundant data accumulated by electric power companies in the future.

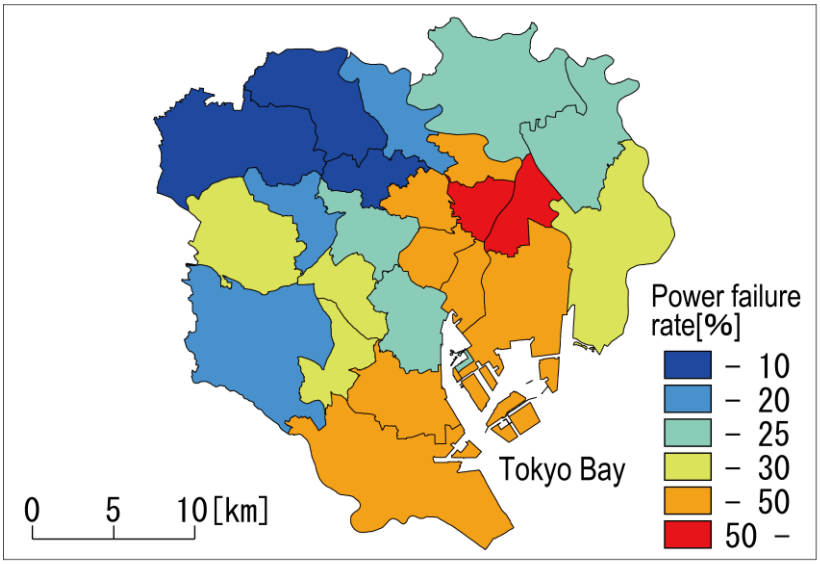

Figure 5. Power failure rate by ward

Elevator stall model

Elevator stall occurrence was predicted using statistical data for the installation of elevators in buildings at least four stories high (Table 3) (Statistics of Japan, 2013) with random numbers to estimate the numbers of buildings at least four stories high actually containing elevators. Next, statistical data for the occurrence of elevator stall as it varied with earthquake severity (Table 4) (Tokyo Metropolitan Government, 2012) were used in combination with random numbers and the estimated earthquake severity in each location to calculate the elevator stall occurrence rate. The parameter values shown in Tables 3 and 4 are obtained from past earthquake disaster damage surveys. Although the progress of elevator technology has been remarkable in recent years, the elevators installed in existing buildings are based on old technology. Therefore, these parameter values are considered to be generally appropriate.

Table 3. Elevator installation rate by the floor number of building

Number of stories	4 stories building	5 stories building	6 or more stories building
Installation rate of elevator	16.3	73.2	100.0

Table 4. Rate of elevator stall

Seismic intensity	Less than 4	Lower 5	Upper 5	Lower 6	Upper 6	7
Rate of elevator stall	0 %	1 %	8 %	15 %	20 %	25 %

CONSTRUCTION OF EVACUATION BEHAVIOR MODEL

Outline of evacuation behavior model

Figure 6 provides an outline of the calculation process of the evacuation behavior model. First (1), the physical damage models in the previous section were used to create an estimate for each building with respect to building damage, fire damage, water supply failure, power failure, and elevator stall. Next, (2) it was estimated whether users of the buildings with at least one of those damage types would seek to evacuate (whether to evacuate). When it had been determined that the users would evacuate, (3) the clock time when the users begin to leave (evacuation time) was estimated. Simultaneously, (4) the damage factors that were the users' reasons to evacuate (evacuation factors) were determined. Additionally, (5) the shelter that was the destination for evacuating was selected, and (6) the clock time of arrival at the shelter (evacuation completion time) was determined.

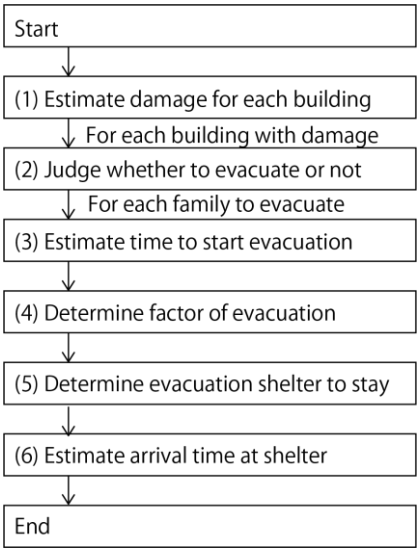

Figure 6. Calculation process of evacuation behavior model

Determination as to whether to evacuate

Statistical data on the variation in the rate of evacuation with the type of physical damage (Table 5) (Tokyo Metropolitan Government, 2015) were employed with random numbers to estimate whether the users of each building would decide to evacuate. This calculation was performed for each damage type in the case of any building that had been determined to receive more than one type of physical damage, and if either calculation yielded a decision to evacuate, the evacuation was assumed to occur. The parameter values shown in Table 5 are obtained from past earthquake disaster damage surveys conducted by Tokyo Metropolitan Government. Evacuation rate is dependent on many factors which include the degree of disaster damages, the local characteristics, time and season. It is therefore difficult to analyze the compatibility of these values for other regions. Detailed analysis on evacuation rate should be scrutinized in the future.

Table 5. Evacuation rate by physical damage

Elevation Factor	Evacuate	Not evacuate	Unknown
Total collapse / fire loss	100.0	0.0	-
Half collapse	50.3	49.7	-
Power / water-supply failure	45.4	33.0	21.6
Elevator inoperative	10.7	69.5	19.8

Next, using the estimate of damage by the Tokyo Metropolitan Government (Tokyo Metropolitan Government, 2015), the building users who have been determined to evacuate were sorted into two groups, those who sought refuge in a shelter (shelter residents) and those who sought refuge in regions outside the affected region (the Tokyo Metropolis) struck by the earthquake, typically at the homes of relatives or friends (refugees). These groups are estimated to show a 65:35 ratio in a population. When buildings were single-family houses, however, this population was assumed to all seek refuge in a shelter together, with a probability of 65%. When buildings were complex housing, 65% of the population was assumed to seek refuge in a shelter and the other 35% of the population was assumed to become refugees.

Determination of evacuation time and evacuation factor

Buildings that have taken serious structural and fire damages are no longer inhabitable, so users must evacuate immediately. However, users can afford to wait for some period of time before leaving when their building has lost “lifelines” such as electric power or water. Functions were formulated (Fig. 7) to express the relationship between the time elapsed after a disaster and the rate of evacuation from the results from a questionnaire and

surveys taken after the Kumamoto Earthquake (Ogino et al., 2016, 2017a; Institute for Human Diversity Japan, 2018).

When building users had multiple reasons to leave, the evacuation times were calculated using Fig. 7, and the reason driving the earliest evacuation was considered the evacuation factor. Additionally, the network distance was estimated by the shelter selection model described below at 12 times the straight-line distance from the building to the shelter. This was converted to travel time to find the evacuation completion time.

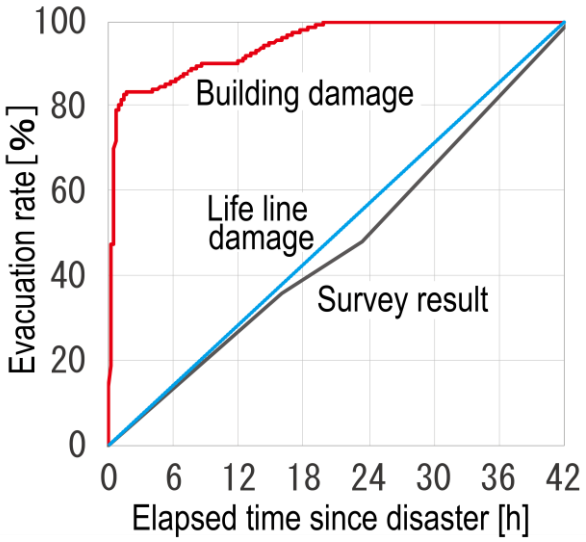

Figure 7. Relationship between elapsed time since disaster and evacuation rate

Shelter selection models

Three models (Voronoi model, Huff model, and logit model) were constructed to describe the evacuees' process of selection of a shelter (shelter selection models), taking the factors affecting selection behavior into account, and were then validated.

In the Voronoi model, the local area was Voronoi-divided in the vicinity of the Voronoi site, and the evacuees were assumed to select the shelter (site) in their own Voronoi region. In other words, this model assumed that they selected the nearest shelter.

Sakata (2000) explained shelter selection behaviors in Nada Ward of Kobe City after the southern Hyogo Prefecture earthquake using the Huff model. The rate of selection of shelters was described by the explanatory variables of shelter scale and distance from the evacuees' homes to the shelter. This model showed good descriptive power. The shelter scale is expressed in this study by the building area [m^2]. The distance resistance parameter was set at the value of 4.15 estimated in the studies by Sakata et al. (1997).

In the logit model, the scale of the shelter (building area), distance from an individual's home to the shelter, and the difference in elevations between home and the shelter location (shelter elevation − home elevation) were the characteristic variables for explaining the utility of the shelters. A descriptive variable was also added to the characteristic function in order to incorporate familiarity with the shelters. This variable had the value of 1 when the shelter was an elementary school and the home was in that school's district, and 0 otherwise.

In the confused situation after the occurrence of a huge earthquake, it is difficult to collect information on the congestion situation of each evacuation center, and it is also extremely difficult to continuous stream of information coming to people regarding what shelter is busy. Therefore, in this study, we assumed that people are blind to how busy a shelter is throughout the whole earthquake. However, since this information affects the behavior of evacuees, we need to investigate effects of providing such information on the severity of crowding at each shelter in the future.

Validation of Shelter Selection Model Using Data from Southern Hyogo Prefecture Earthquake

We attempted to validate this model using the household data of individuals from a certain area of Nada Ward,

Kobe City who had used the shelters listed in Table 6 following the devastating earthquake in Kobe (southern Hyogo Prefecture earthquake of 1995), using the data gathered in surveys by Sakata (2000) and Tokyo Metropolitan Government (2018). Table 6 and Fig. 8 show the building areas of the seven shelters with the numbers of households staying there and the spatial distribution of the shelters, respectively. We traced the results of their surveys for the location of houses of households using the shelters and shelters they selected. We treated the shelters in Iwaya Community Welfare Center, Nishinada Kindergarten, and Iwaya-Kita Park as a single entity, because they were located quite close together and were managed as one by the same authority.

Table 6. Building area and the number of households by evacuation shelter

No.	Name of shelter	Area of shelter [m^2]	Number of households actually evacuated
1	Iwaya community welfare center	987	117
2	Hieda elementary school	3,049	267
3	Fukuzumi elementary school	1,299	151
4	Maya elementary school	1,818	248
5	Seiyo-higashi handicapped children's school, etc.	2,532	472
6	Kobe high school	2,187	368
7	Oji sport center	3,925	234

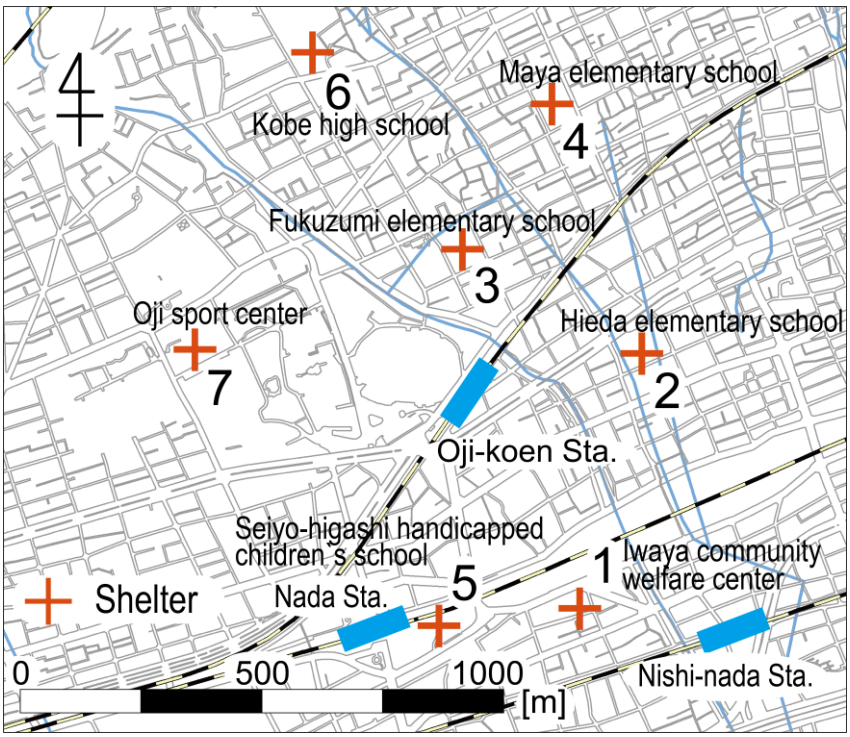

Figure 8. Spatial distribution of evacuation shelters (Kobe Earthquake, 1995)

Table 7 provides the fitting rates for each model, which indicates what percentage of the total sample was correctly estimated by the model. Even the quite simple Voronoi model accurately predicted the shelter chosen by the evacuees and is an effective method for simply describing shelter selection behaviors. The Huff model also boasted a high fitting rate. The reader can see that distance resistance has a strong effect on shelter selection behavior.

Table 7. Fitting rate of each model for the data of Kobe earthquake

	Fitting rate [%]	Likelihood rate
Voronoi model	59.4	
Huff model	56.8	
Logit model (1) [A, B, C,]	61.4	0.348
Logit model (2) [A, B, , D]	58.9	0.390
Logit model (3) [A, , C, D]	31.0	0.076
Logit model (4) [, B, C, D]	56.8	0.384
Logit model (5) [A, B, C, D]	57.8	0.398

Table 8 shows the standardized estimated parameters for the logit model. As seen in the Huff model, the larger a shelter was and the closer it was to home, the more likely it was to be chosen. The location of the home in a school district was also a statistically significant parameter; the role of elementary schools, a regional center as an ordinary and familiar location was apparent here. There was a positive value for the standardized estimated parameter of elevation difference, and this may be because the region examined here had a high elevation with relatively little damage.

Residents do not always know the locations of all the public facilities in their areas. However, everyone knows the location of the primary school, and this is especially true for those who were born and grown up in the area. As a core facility of the local community, an elementary school is expected to play an important role not only in normal times but also in emergencies. The results of analysis showed that the conventional facility selection behavior model, whose explanatory variables are the distance to facility and the scale of facility, could not explain enough. More precise estimation will be expected if we specify the residential areas assigned to each school district and incorporate it into the model.

Table 8. Standardized estimated parameters of logit model based on Kobe Earthquake

Road width	Building area	Distance	School district	Elevation
Logit model (1)	0.322**	-1.84**	0.124**	-
Logit model (2)	0.283**	-2.39**	-	0.949**
Logit model (3)	0.253**	-	0.423**	0.0521
Logit model (4)	-	-2.31**	0.150**	1.04**
Logit model (5)	0.289**	-2.30**	0.162**	1.00**

**: Statistically significant at 1%

Figure 9(a) presents the actual shelter selection behavior and Fig. 9(b) presents the selection behavior predicted by the logit model (1) (characteristic variables: shelter area, distance, and school zone). The reader can see that the predicted spatial distribution of the selection behaviors was generally correct.

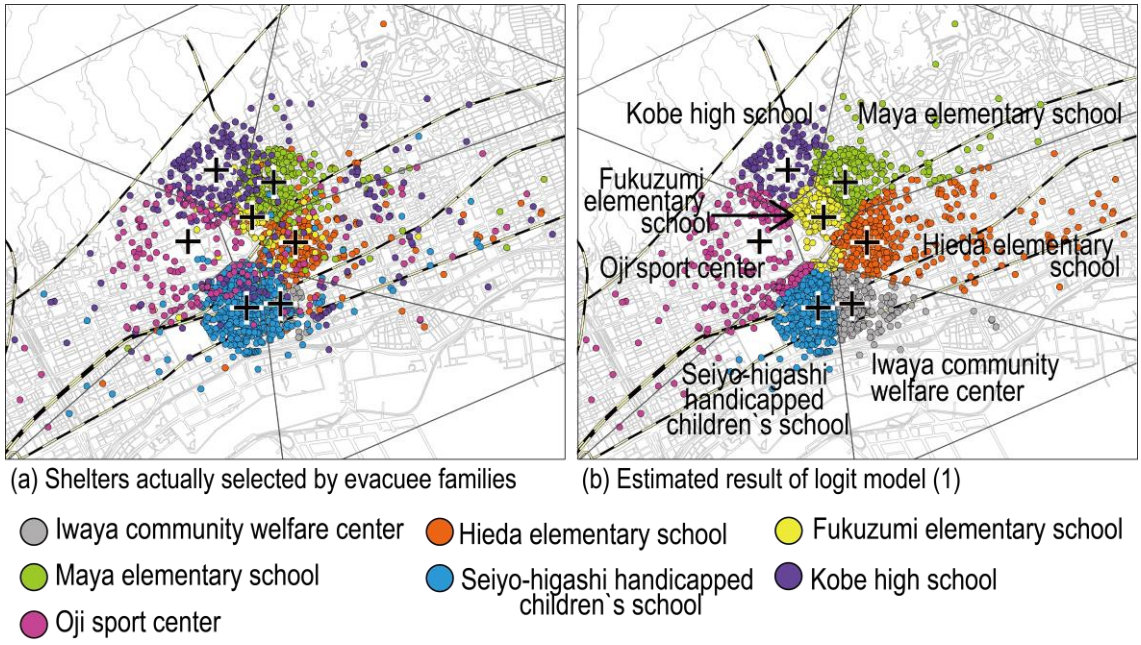

Figure 9. Actual evacuation shelter selection behavior and estimation result of logit model

However, the fitting rate for evacuees who had no shelter near their homes tended to diminish as the evacuation distances increased (Fig. 10). This was probably due to factors not covered by the above variables, for example, the severity of crowding at a shelter, the quality of a shelter environment, the surrounding environment, and the presence of people known to the evacuees. The severity of crowding at each shelter (congestion degree) is described as a value obtained by dividing the number of shelter residents by that of the assumed number in a disaster prevention planning.

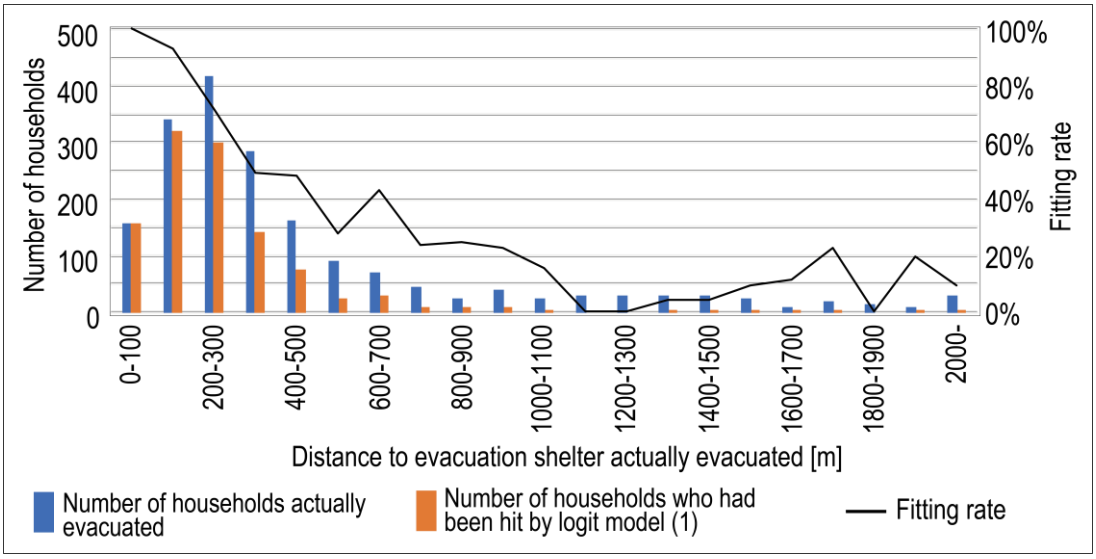

Figure 10. Fitting rate according to distances to evacuation shelters

Validation of Shelter Selection Model using Kumamoto Earthquake Data

The shelter selection model constructed in the previous section was tested to validate whether it would correctly predict such behaviors in a different major earthquake. Survey data from the Kumamoto Earthquake (2016) were used to check each model. The parameters for each model were those used in the survey of southern Hyogo Prefecture earthquake of 1995 as-is. This also validated the robustness of those parameters.

The main areas surveyed were Higashi-ku of Kumamoto City and Mashiki Town of Kamimashiki District, both of which sustained the heaviest damages during the Kumamoto Earthquake. A questionnaire was created regarding evacuation behaviors while seeking shelters (Ogino et al., 2016, 2017a) at that time. Of the 190 households who returned responses, 51 provided their addresses and indicated that they stayed in shelters (not including cars). The 24 shelters used by those households are analyzed here (Fig. 11).

Table 9 shows the fitting rates of each model. Since the fitting rates of the Voronoi and Huff models were over 50%, it is clear that they are simple but effective procedures for predicting selection behaviors. Logit models (1), (4), and (5) boasted fitting rates over 60%, and were considered to show an excellent degree of consistency. Thus, we expect the logit model, which was constructed using the survey data from the southern Hyogo Prefecture earthquake, to describe the shelter selection behaviors after other earthquakes quite well.

Table 9. Fitting rate of each model for Kumamoto earthquake data

	Fitting rate [%]
Voronoi model	54.9
Huff model	56.9
Logit model (1) [A, B, C,]	60.8
Logit model (2) [A, B, , D]	58.8
Logit model (3) [A, , C, D]	33.3
Logit model (4) [, B, C, D]	60.8
Logit model (5) [A, B, C, D]	60.8

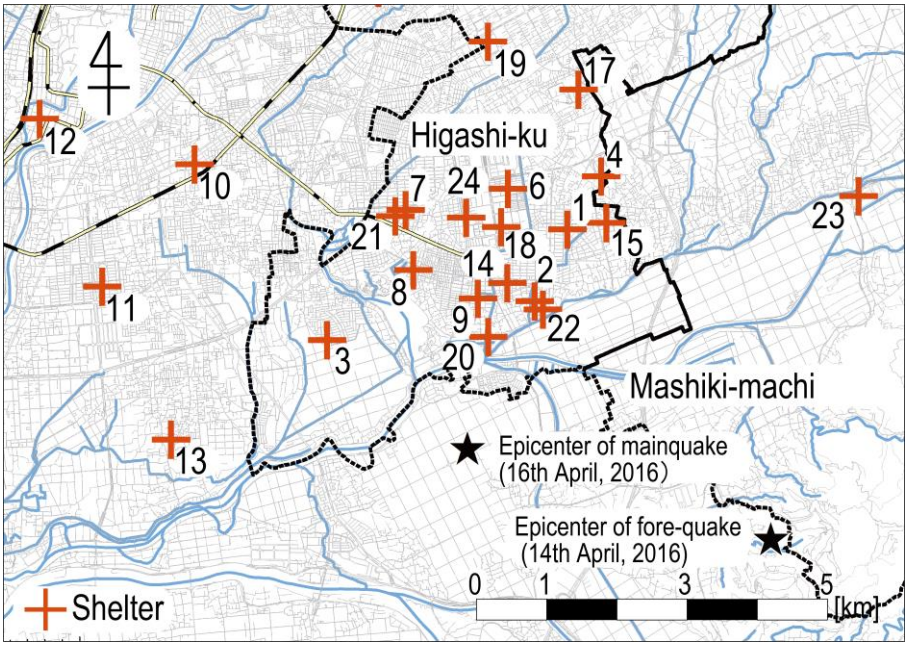

Figure 11. Spatial distribution of target evacuation shelter (Kumamoto earthquake)

ESTIMATE OF CROWDING IN SHELTERS AFTER MAJOR EARTHQUAKE WITH EPICENTER IN TOKYO

Simulation Assumptions

In this study, 100 cases of varying physical damage (building damage, fire damage, water supply failure, power failure, elevator stall) were created on the assumption that a northern Tokyo Bay earthquake of magnitude 7.3 struck at 6:00 on a winter evening while the wind was blowing from the north at 8 m/s. Simulations were carried

out of the evacuation behaviors using the series of models described through the preceding section, encompassing the various physical damage cases, for the two days (48 hours) following the disaster in the Tokyo ward area (below, evacuation behavior simulation). Logit model (1) was employed for this.

Let's begin with an overview of the method and the data used for the various estimates of physical damage. The building data are from a 2011 survey of the current conditions of buildings in the Tokyo ward area and covered some 1,748,615 structures. For information about shelters, the National Land Numerical Information Download Service (2012) (Ministry of Land, Infrastructure, 2018) was used. These data describe the evacuation shelters shown in the regional disaster plan created by the Tokyo Metropolitan Government and those of its component cities and wards, as specified by the Basic Act on Disaster Management.

The official number of all shelters in the Tokyo Metropolis is 3,809, but no precise number has ever been announced for how many people these can accommodate. Assuming that the capacity of each shelter is proportional to the scale of the facility, we (1) found the floor area of each facility from a survey of current uses of land and buildings (2011), and then (2) distributed the total announced capacity of evacuees (3,280,000) among the announced shelter proportionally to their floor areas in order to estimate the capacity of each individual shelter.

It is common to analyze the turmoil immediately after the disaster using a transient population distribution (daytime population distribution), since it is unknown what time a large earthquake will occur. For this purpose, we need to use the data on transient occupants of the Tokyo urban area, which can be estimated for each building and each hour of the day using person-trip survey data (PT data) taken in the Tokyo Metropolis and residential floor area data (Osaragi, 2020; Osaragi and Kudo, 2021). However, it is expected that transient occupants away from their homes at the time of a disaster will return to their households and then evacuate with their family. Therefore, as part of the process of estimating the number of evacuees, the numbers of that group were calculated using the spatial distribution of the population at night time.

Figure 12 shows the ward-wide status of the seismic retrofitting of water pipelines for each ward of Tokyo (as of end FY2015) (Bureau of Waterworks, 2018). It was not stated which of the pipes have been retrofitted, but generally, the mains buried beneath the widest streets are the most important water pipelines, and are the most likely to be retrofitted first. The pipes were identified in order of largest diameter and it was assumed that the pipes had been already retrofitted in this order until the indicated seismic retrofitting rate was reached.

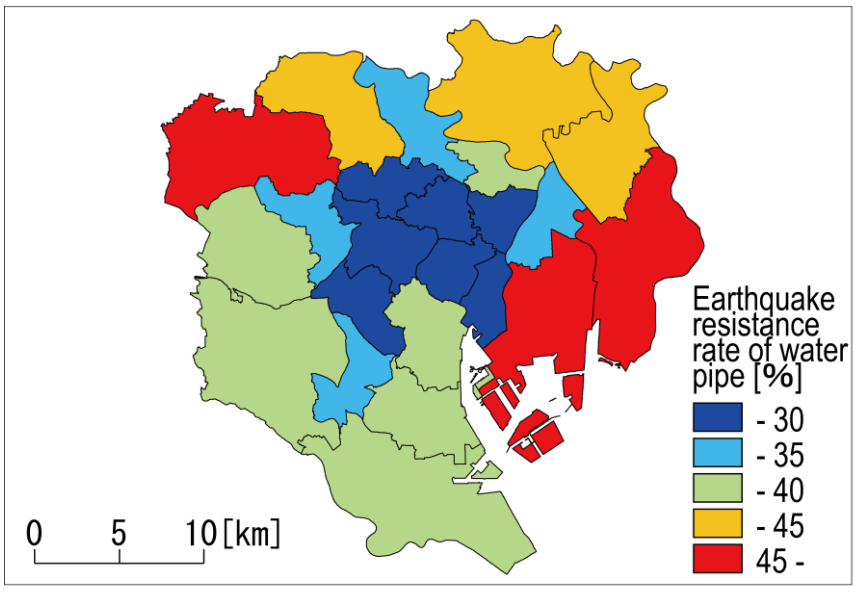

Figure 12. Status of earthquake resistance of water pipeline for each ward

Results of Evacuation Behavior Simulation

Numbers of shelter residents, by evacuation factor

Figure 13 shows the mean number of shelter residents, grouped by evacuation factor, from the results of 100 runs of the evacuation behavior simulation. It is estimated that about 2 million among the ward population will become

shelter residents. About 700,000 of these are accounted for, each, by the factors of building damage and water supply failures; thus, these two are the main evacuation factors. They are followed by estimated numbers of 450,000 due to power failure, 50,000 due to fire damage, and 30,000 due to elevator stall.

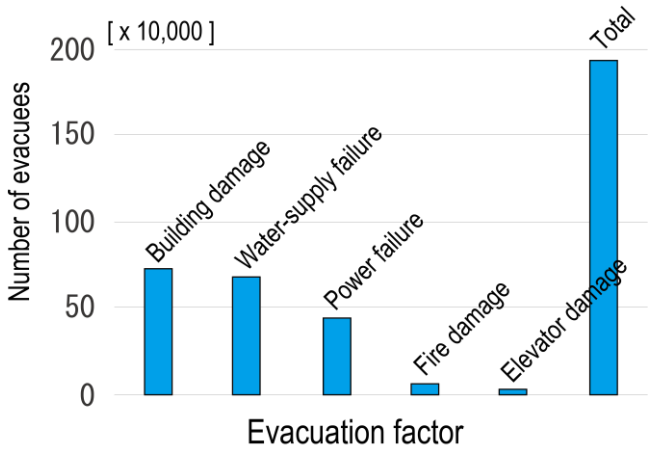

Figure 13. Number of people staying at shelters by each evacuation factor

Severity of crowding at shelters

The severity of crowding in a given evacuation shelter is defined as the ratio of the shelter residents to the estimated capacity of the shelter (estimated in the evacuation behavior simulation). Figure 14 shows the fraction of shelters where the severity of crowding exceeds 1.0 and how the number of residents changes with time. The number increases sharply just after the disaster, due to building and fire damages. At 12 hours after the disaster, the total number of shelter residents surpasses 1 million, and the severity of crowding surpasses 1.0 in about 20% of the shelters. After 24 hours, the severity of crowding exceeds 1.0 in nearly 40% of the shelters, and after 48 hours, this is reaches 1.0 in over 50%.

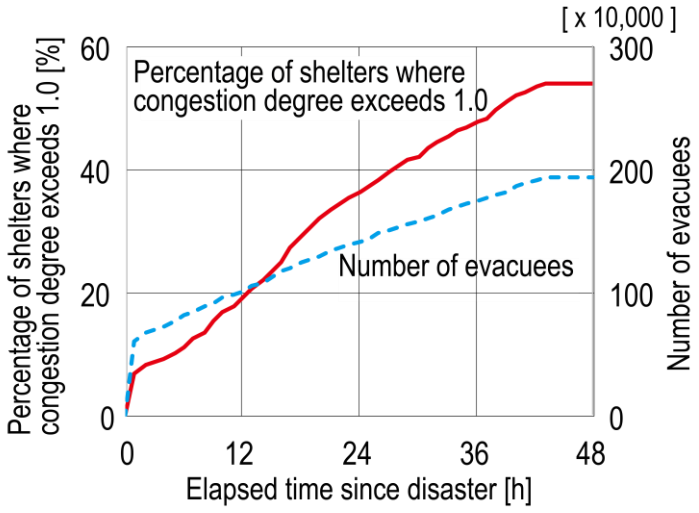

Figure 14. Trends of congestion situation and the number of people in evacuation shelters

Figure 15 provides the number of shelter residents in each shelter 48 hours after the disaster and the spatial distribution of crowding. The severity of crowding exceeds 1.0 in many of the shelters in east and south Tokyo. Notably, Arakawa Ward, Sumida Ward, and Ota Ward have many shelters where the severity of crowding is over 3.0.

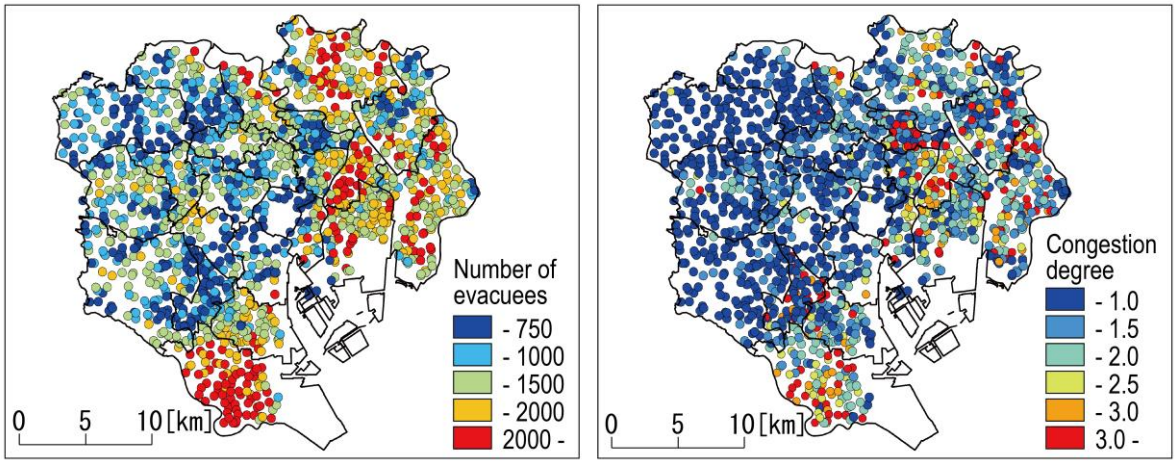

Figure 15. Number of people staying at evacuation shelters and congestion degree of evacuation shelters (48 hours after the disaster). Congestion degree is described as a value obtained by dividing the number of shelter residents by that of the assumed number in a disaster prevention planning.

Spatial distribution of numbers of shelter residents

Figures 16(a)–(e) display the numbers of shelter residents by evacuation factor and residential location (500 m grid cell). This confirms that in the regions described above where crowding in the shelters is worst, building damage and water supply failure are the reasons for the bulk of evacuees (Figs. 16(a) and (b)). Relatively few people are driven out of their homes by fire (Fig. 16(d)), but the numbers of evacuees were locally high in densely built residential areas with wooden construction. Over 800 residents had to leave a residential area in a single 500 m grid cell due to fires. Even urban areas that had relatively little in the way of building damages or water supply failures contained some regions where elevator stalls in high-rise condominiums and other buildings forced residents into shelters (Fig. 16(e)).

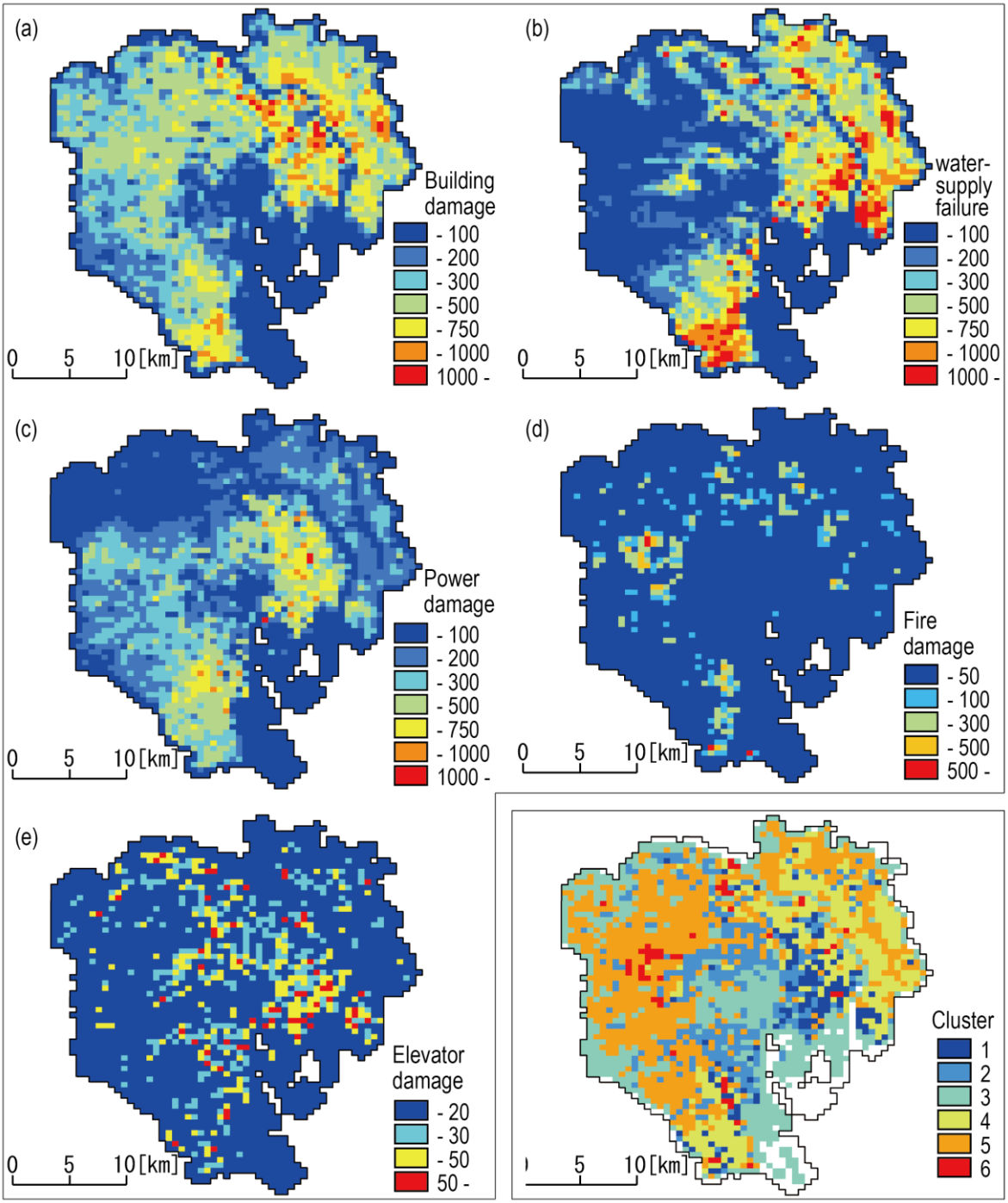

Figure 16. Number of evacuees due to building damage, water supply failure, fire damage, elevator stall

Figure 17. Regional classification result by the number of evacuees due to evacuation factors

Classification of areas by evacuation factor

The regions were classified using non-hierarchical cluster analysis (k-means clustering; Buttigieg and Ramette, 2014). The reasons for evacuation depend largely on the local characteristics of the evacuation factors. Therefore, by classifying evacuees from the viewpoint of evacuation reasons, we attempted to clarify the local uneven distribution characteristics of evacuees and their evacuation reasons. Namely, we attempted to clarify what the spatial distributions were with respect to the evacuation factor. A total of 2,424 grid cells were examined. Figure 17 shows how the regions were classified into six clusters based on the number of shelter residents and Fig. 18 shows how the factors varied among the clusters. Cluster 1 comprised regions where most shelter residents had

multiple reasons for leaving, including water supply failures, power failures, and elevator stalls (138 cells). Cluster 2 comprised regions where most shelter residents had left because of elevator stalls (358 cells). Cluster 3 comprised regions containing few residents and extremely few shelter residents (655 cells). Cluster 4 comprised regions whose shelter residents had been driven out by building damages and water supply failures (371 cells). Cluster 5 comprised regions with relatively few shelter residents (850 cells). Finally, Cluster 6 comprised regions whose residents had been driven to shelters by fire damage (52 cells).

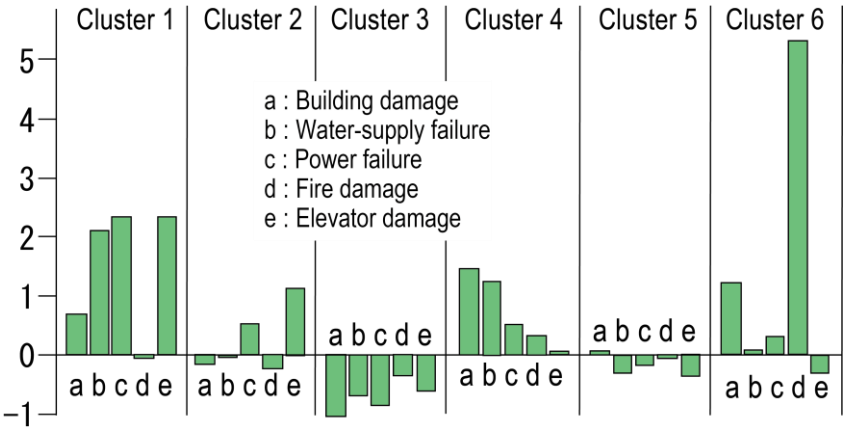

Figure 18. Average number of people in evacuation shelters in each class (standardized value)

INVESTIGATION OF MEASURES TO REDUCE CROWDING BY SEISMIC RETROFITTING OF WATER PIPES

Definition of seismic retrofitting priority factor

Efficient methods of seismically retrofitting water pipes were examined to see how well they could be predicted to reduce the number of shelter residents due to water supply failures. The most efficient way to minimize such evacuees' numbers is to prioritize seismic retrofitting of the pipes by the numbers of evacuees most likely to be forced out if they fail. Therefore, we define the seismic retrofitting priority factor I_L (Fig. 19) as the number of shelter residents who would be forced out of their buildings by the failure of a pipe L. Next, we validate the plausibility of the method of beginning the retrofits at locations with the highest value of I_L.

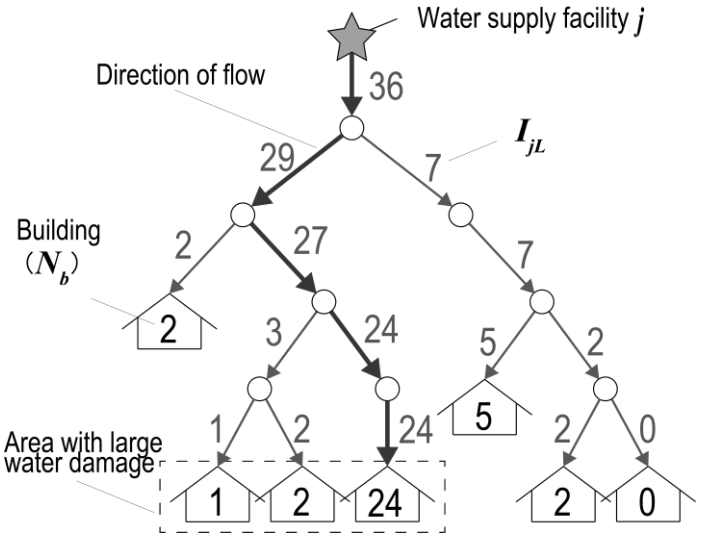

Figure 19. Calculation method for earthquake resistance importance factor IL

Specifically, the following procedure is followed. (1) The results of 100 evacuation behavior simulations are used to calculate the mean number of shelter residents N_b who leave building b because of a water supply failure. (2) The values of N_b for a given building are added to I_{jL} for each pipe L encountered as the water supply route from

the given building upstream to each water supply facility j that can supply it is traced. (3) Once calculation (2) is performed for every building, the expected value I_{jL} for the number of shelter residents who would appear due to a rupture in pipe L connected to facility j. (4) I_{jL} is calculated for every facility j, and the seismic retrofitting priority factor I_L is applied to the pipe L, which has the maximum value I_{jL} for all the facilities.

Effectiveness of Seismic Retrofitting of Water Pipes when using Seismic Retrofitting Priority Factor

The Tokyo Metropolis has set the numerical goals of seismic retrofitting of about 5,000 km of water pipes over the next 10 years from this writing. This will raise the seismic retrofitting rate from the 29% as of end FY2011 to 54% as of end FY2022. This value was used as reference in our simulation; excepting the pipes assumed to be already retrofitted as described in Section 4, the appropriate fraction of pipes in the Tokyo Metropolis with the highest I_L values (the top R %) of all the un-retrofitted pipes (total length, 18,816 km) were assumed to have been retrofitted so as to meet the above-stated goals. Specifically, it was assumed that an additional R % of the pipes had been retrofitted, beginning with those having the highest I_L, and 100 simulations with varying physical damages were performed, as done in Section 4. The simulations covered the 48 hours (2 days) following the occurrence of the earthquake.

Figures 20(a)–(d) show how the water supply failure varied as the value of R was gradually increased. Beginning at the end of 2015, with the base seismic retrofitting rate (R = 0.0%, Fig. 20(a)), the reader can see that liquefaction (Fig. 3) determined the spatial distribution of the rate of water supply failure. This rate can be seen to have improved over the entire metropolis when the extent of retrofitting R had reached 0.25% of the water pipeline (about 47 km of pipe), but there remained many areas in which the rate of water supply failure still exceeded 80% (Fig. 20(b)). At R = 2.0% (about 376 km), the rate of water supply failure dropped below 10% in the west part of the Tokyo ward area, and was no more than 50% in nearly all the portions of east and south part of the area, where serious water supply failure has been predicted (Fig. 20(c)). At R = 10.0% (about 1,882 km), the rate of water supply failure is about 10% throughout the Tokyo ward area; which indicates that it is possible to bring about an efficient and effective reduction of the rate of water supply failure (Fig. 20(d)). However, a close examination of Fig. 20(d) reveals that the high rates of water supply failure in locations distant from water supply facilities remain unsolved. This is due to the high cumulative probability of a pipe rupture somewhere in the long route from a water supply facility to such a location and to the low I_L value of pipes near such a location, which corresponds to the outer edge of the region supplied by a facility. These issues are due to the low priority assigned to the local seismic retrofits.

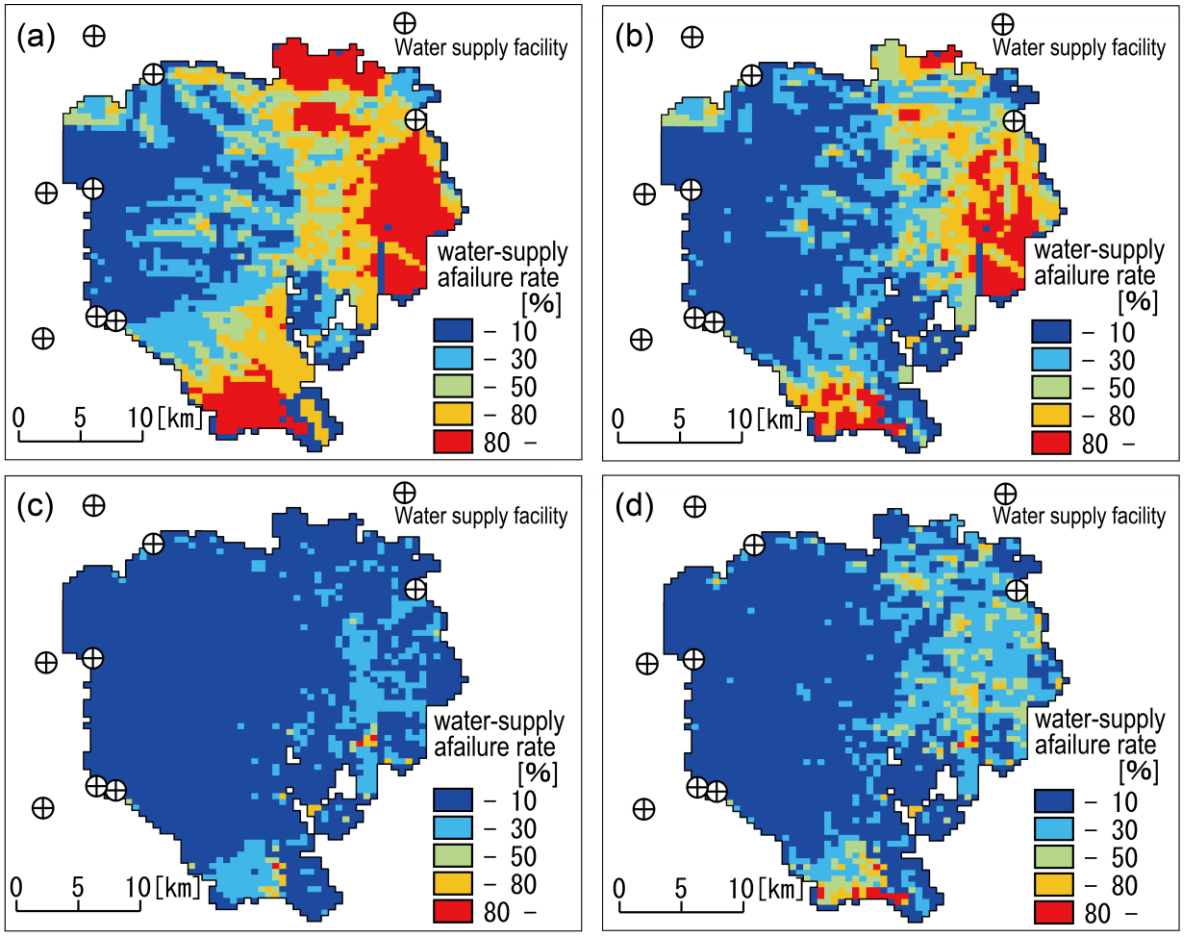

Figure 20. Effects of earthquake resistance improvement of water pipeline

Figure 21 shows the variation in the number of buildings having water supply failure, in the number of shelter residents evacuating due to water supply failure, and in the number of shelters having a severity of crowding over 1.0 at 48 hours after the disaster, with the seismic retrofitting rate. The objective of seismic retrofitting of water pipeline is to increase the pipe's strength and its deformability so that the seismic retrofitting enables it to withstand more weight and better stand up to the crushing forces released during earthquakes, ground motion, and soil failure. The reader can see that when R was 0.25% (about 47 km), this eliminated water supply failures in over 230,000 buildings, and the shelter resident population due to that cause was reduced by about 240,000. At R = 2.0% (about 376 km), the shelter resident population due to water supply failure was reduced to about one-fourth what it had been in the current condition (R = 0.0%), (to about 170,000) and the severity of crowding had fallen below 1.0 in about 250 shelters. At R = 10% (about 1,882 km), the shelter resident population due to water supply failure had shrunk to about 70,000. This indicates that it is possible to bring about an efficient and effective reduction of the shelter resident population who have evacuated due to water supply failure by calculating the seismic retrofitting priority factors I_L for all the water pipes and using these values to perform retrofits on the pipes with the greatest I_L values first.

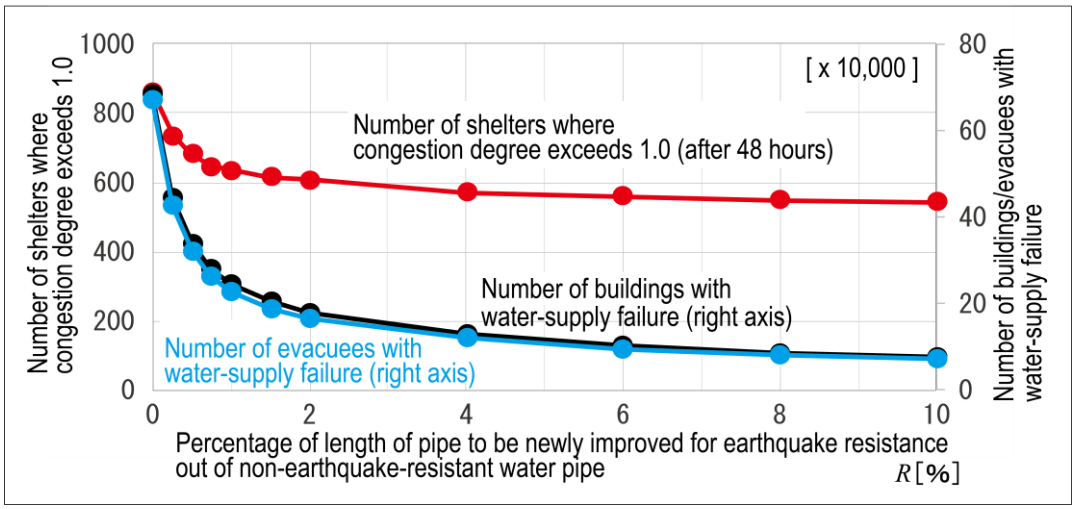

Figure 21. Relationships between earthquake resistance rate of water pipeline and the number of buildings of water-supply failure, number of evacuees, and congestion degree of shelters

SUMMARY AND CONCLUSIONS

It is essential to predict how severe crowding will be at evacuation shelters after a major earthquake occurs in order to forestall confusion and trouble at shelters. However, it is difficult to anticipate the crowding at shelters, as this will depend on the local levels of physical damage, on the numbers of shelter residents, on the scale of each shelter itself, and particularly on the spatial distribution of all these factors. In this study, evacuation behaviors due to physical damage after a major earthquake were modeled assuming a northern Tokyo Bay earthquake (M7.3) occurs. The severity of crowding at every shelter in the Tokyo ward area was estimated, and countermeasures were examined for their effectiveness in reducing congestion.

First, a model was constructed to estimate the physical damages (building damage, fire damage, water supply failures, power failure, elevator stalls) occurring in each individual building. Next, a model was constructed to estimate whether or not an individual or family would decide to seek shelter, and a shelter selection model was constructed to predict which shelter would be chosen. Using survey data from the southern Hyogo Prefecture earthquake, the most influential parameters for the shelter selection model were shown to be the scale of the shelter, its distance from the evacuee's home, and whether the shelter was located in the same school district as the evacuee's home. These parameters were applied to survey data from the Kumamoto Earthquake, and the results were consistent with the results in the southern Hyogo Prefecture earthquake.

Next, a simulation was carried out using the evacuation behavior model for people in the Tokyo ward area over the first 2 days (48 hours) after a northern Tokyo Bay earthquake (M7.3) has occurred. The simulation showed that about 2 million people throughout the area would seek shelter, consisting mainly of about 700,000 each due to building damage and to water supply failure. Additionally, at 48 hours after the earthquake, over half of the shelters would be housing more residents than they are intended for. This crowding was predicted to be particularly severe in Arakawa Ward, Sumida Ward, and Ota Ward, where the severity of crowding would exceed 3.0.

Lastly, focusing on water supply failure, which is one of the chief reasons for seeking shelter, a calculation was made of the expected number of people who would seek shelter due to pipe rupture (the seismic retrofitting priority factor) for every water pipe. It was then calculated how effectively shelter crowding would be reduced by replacing the pipes in descending order of their seismic retrofitting priority factor to validate this approach. This demonstrated that replacing 0.25% (about 47 km) of the un-retrofitted but most critical pipe would reduce the number of shelter residents by about 240,000, while replacing 2.0% (about 376 km) of pipe would further reduce shelter residents to about 170,000. This indicates that even small but well-directed efforts at retrofitting water pipe may yield dramatic results in reducing the numbers of evacuees.

One of the most important findings in this study is that the measures of Tokyo Metropolitan Government have calculated only the number/size of evacuation shelters that are needed in the entire area of Tokyo, and have never calculated it according to the information of space and time when a disaster occurs. We demonstrated in this paper that the importance of spatiotemporal characteristics of necessary evacuation shelters should never be neglected.

Also, Tokyo Metropolitan Government has considered only the people who evacuate to shelters due to the property damages caused by collapsed building or fire spreading. We demonstrated in this paper that more people would have potential to evacuate when the water supply failure, electric failure, or elevator stalls. These new findings demonstrated that we should consider measures while assuming the number of evacuees, the required number/size of evacuation centers will vary greatly according to the location of earthquake epicenter and the elapsed time since the occurrence of a disaster. In this paper we have proposed the framework to address these issues which have never been discussed theoretically nor practically.

Next, let us consider themes for future studies. This study provided estimates for power failure and elevator stalls in individual buildings. However, power failure usually occurs simultaneously over wide areas. Additionally, "elevator stall" covers a great variety of issues, depending on the year the elevator was installed and its functions. These topics must be examined with greater precision in the future. Furthermore, the seismic retrofitting priority factor must be calculated with respect to other considerations than just shelter resident population because it is essential to prioritize water service to hospitals and other vital facilities. This must also be addressed in future investigations.

The proposed models and methods are weak in generality because they are estimated based on specific dataset environment. The authors believe that a model that can respond to an emergency needs to have generality. However, examples of practical usage might be often weak in its generality. This is because model's parameters are often dependent on the local characteristics/environment, or vary dramatically according to the time or seasons when a disaster occurs. Another reason is that there are very few cases of devastating earthquakes as envisioned in this research occurred in a large city like Tokyo, and corresponding data are also not available. We have carefully investigated domestic and overseas research, but there are very few literatures to secure generality of models. Especially, it's very difficult to obtain the data about human behaviors in the immediately after the occurrence of a devastating earthquake. This fact results in lacking of generality of models even in previous research. For these reasons, we dared to use the limited data and theories derived from researches on the Kobe earthquake (1995) and Kumamoto earthquake (2016) occurred in recent years. Namely, in this study, rather than focusing on the generality of a model itself, we examined what we need to consider in crowding evacuation shelters, how to address this difficulty, and how to reduce the risks, by assuming the earthquake directly beneath Tokyo. Having so said, we would like to address the generality more in detail in our future work, since aiming for generality is one of the meaningful goals for academic research.

ACKNOWLEDGMENTS

The authors wish to express their sincere thanks for Tokyo Metropolitan Government and Tokyo Fire Department for providing valuable data. This report is an expanded and corrected version of Osaragi et al. (2019).

REFERENCES

Buttigieg, PL. and Ramette, A. (2014) A Guide to Statistical Analysis in Microbial Ecology: a community-focused, living review of multivariate data analyses, *FEMS Microbiol Ecol.* 90, 543–550.

Bureau of Waterworks (Tokyo Metropolitan Government) (2018) *https://www.waterworks.metro.tokyo.jp/suidojigyo/shinsai/suidoukanro10.html* (accessed 2018-01-20)

Hirokawa, N. and Osaragi, T. (2016) Earthquake Disaster Simulation System, Integration of Models for Building Collapse, Road Blockage, and Fire Spread, *Journal of Disaster Research*, 11(2), 175-187.

Hirokawa, N. and Osaragi, T. (2017a) Fire-spread Indices Based on Large-scale Simulation in Case of Multiple Simultaneous Fires and its Application for Assisting Firefighters, *Journal of Architecture and Planning* (*Transactions of AIJ*), 82(732), 301-310.

Hirokawa, N. and Osaragi, T. (2017b) Availability of Hydrants after a Large Earthquake: Simulation Analysis on Water Outage, Fire-spreading, and Firefighting, *Journal of Architecture and Planning* (*Transactions of AIJ*), 82(739), 2185-2195.

Institute for Human Diversity Japan (2018) *http://diversityjapan.jp/wordpress/wp-content/uploads/2016/04/kumamoto_report_1-2.pdf* (accessed 2018-01-20)

Iwami, T., Ohmiya, Y., Hayashi, Y., Naruse, T., Takeya, S., Kagiya, K., Itoigawa, E., Kato, T., Shida, K., Hokugo, A. and Takahashi, W. (2006) Development of Evaluation Methods for Fire Spread Risk in Urban Area, *BRI Research Report*, 145, 1-66.

Kobayashi, T., Yamazaki, F. and Maruyama, Y. (2013) Estimation of Water-pipeline Length from GIS Road Network Data, *Journal of Social Safety Science*, 21, 267-274.

Ministry of Land, Infrastructure, Transport and Tourism (2018) National Land Numerical Information Download Service, *http://nlftp.mlit.go.jp/ksj/gml/datalist/KsjTmplt-P20.html* (accessed 2018-02-04)

Murao, O. and Yamazaki, F. (2000) Development of Fragility for Buildings based on Damage Survey Data of a Local Government after the 1995 Hyogoken-Nanbu Earthquake, *Journal of Architecture and Planning* (*Transactions of AIJ*), 65(527), 189-196.

Ogino, K., Osaragi, T. and Oki, T. (2016) Congestion of Shelters after a Tokyo Metropolitan Earthquake, *Papers and Proceedings of the Geographic Information Systems Association* (*CD-ROM*), GIS Association of Japan, 25.

Ogino, K., Osaragi, T. and Oki, T. (2017a) Modeling of Shelter Choice in a Large Earthquake, Summaries of Technical Papers of Annual Meeting, *Architectural Institute of Japan*, E-1, 609-610.

Ogino, K., Osaragi, T., Oki, T. and Hirokawa, N. (2017b) Influence of Regional Characteristics and Water Outage on Congestion of Shelters after a Large Earthquake, *Papers and Proceedings of the Geographic Information Systems Association* (*CD-ROM*), 26.

Osaragi, T. (2020) Estimating Spatiotemporal Distribution of Moving People in Urban Areas Using Population Statistics of Mobile Phone Users Environmental Informatics, EnviroInfo 2020: *Environmental Informatics, Advances and New Trends in Environmental Informatics*, Springer International Publishing, 181-192.

Osaragi, T., Hirokawa, N. and Oki, T. (2015) Information Collection of Street Blockage after a Large Earthquake for Reducing Access Time of Fire Fighters, *Journal of Architecture and Planning* (*Transactions of AIJ*), 80(709), 465-473.

Osaragi, T. and Kudo, R. (2021) Upgrading Spatiotemporal Demographic Data by the Integration of Detailed Population Attributes, 30th International Cartographic Conference (ICC 2021), *Advances in Cartography and GIScience of the ICA*, Copernicus Publications, 3.

Osaragi, T., Ogino, K., Hirokawa, N. and Oki, T. (2019) Congestion Degree of Evacuation Shelters Under the Assumption of Tokyo Bay Northern Earthquake, *Journal of Architecture and Planning* (*Transactions of AIJ*), 84(760), 1521-1530.

Sakata, K., Kashihara, S., Yoshimura, H. and Yokota, T. (1997) A Study on the Range of Shelters in Kobe Earthquake Disaster: A case study of the shelters in Nada ward in Kobe city, *Journal of Architecture and Planning* (*Transactions of AIJ*), 62(501), 131-138.

Sakata, K. (2000) Characteristics of the Transition in the Number of Refugees in Shelters and the Behavior of Choosing Shelters in the Earthquake Disaster: A study on the planning of shelters in regional plans for prevention of disasters, *Journal of Architecture and Planning* (*Transactions of AIJ*), 65(537), 141-147.

Statistics of Japan (2013) Housing and Land Survey 2013: https://www.e-stat.go.jp/stat-search/files?page=1&toukei=00200522&tstat=000001063455 (accessed 2018-01-20)

Seto, T., Kashiyama, T. and Sekimoto, Y. (2016) The Evacuation Center Estimation for Human Congestion using Positioning Data of Mobile Phones on the 2016 Kumamoto Earthquake, *Papers and Proceedings of the Geographic Information Systems Association* (*CD-ROM*), GIS Association of Japan, 25.

Tokyo Fire Department (1997) Provision and Elucidation of New Factor of Fire and Fire Spread Behavior Considering Inland Earthquakes, *Report of Fire Prevention Council*.

Tokyo Fire Department (2001) Development and Application of Evaluation Method for Preventing Ability of Earthquake Fire, *Report of Fire Prevention Council*.

Tokyo Fire Department (2005) Provision and Elucidation of Risk Factor after Large Earthquake in Civilization, *Report of Fire Prevention Council*.

Tokyo Metropolitan Government (2012) Estimation of Earthquake Damage in Tokyo (2012), *https://www.bousai.metro.tokyo.lg.jp/taisaku/torikumi/1000902/1000401.html* (accessed 2022-03-05)

Tokyo Metropolitan Government (2018) Disaster Prevention Information, *http://www.bousai.metro.tokyo.jp/bousai/1000026/1000316.html* (accessed 2018-01-20)